

# Improvement of minimum paint film thickness for THz paint meters by multiple-regression analysis

Takashi Yasuda,<sup>1,3</sup> Tetsuo Iwata,<sup>2</sup> Tsutomu Araki,<sup>1</sup> and Takeshi Yasui<sup>1,\*</sup>

<sup>1</sup>Graduate School of Engineering Science, Osaka University, 1-3 Machikaneyama-cho, Toyonaka, Osaka 560-8531, Japan

<sup>2</sup>Department of Mechanical Engineering, University of Tokushima, 2-1 Minamijousanjima-cho, Tokushima 770-8506, Japan

<sup>3</sup>Present address: Central Research Laboratory, Hamamatsu Photonics K.K., 5000 Hirakuchi, Hamakita-ku, Hamamatsu, Shizuoka 434-8601, Japan

\*Corresponding author: t-yasui@me.es.osaka-u.ac.jp

Received 18 April 2007; revised 22 July 2007; accepted 23 July 2007;  
posted 27 July 2007 (Doc. ID 82193); published 18 October 2007

We propose a numerical parameter fitting method to determine the time delay between two temporally overlapped echo pulses in terahertz (THz) tomography measurements. The method is based on multiple-regression analysis with the least-squares method and is applied to decrease the minimum paint film thickness for THz paint meters. Applying multiple-regression analysis to paint thickness measurements is five times more sensitive with regard to the minimum thickness than numerical Fourier deconvolution. We apply the proposed method to determine the optical thickness, geometrical thickness, and group refractive index of dry paint film and wet paint film. The proposed method is useful for decreasing the minimum thickness for a THz paint meter and other THz tomography measurements. © 2007 Optical Society of America

*OCIS codes:* 110.6960, 120.4290, 310.1620.

## 1. Introduction

In the last few decades, terahertz (THz) electromagnetic pulses have received interest as a new probe for nondestructive testing. In addition to excellent transmittance in nonmetal materials, THz pulses provide attractive features for nondestructive testing, such as free-space propagation, extremely low invasion, beam coherence, ultrashort pulse duration, broad spectral width, and the availability of imaging and/or spectroscopy. Of the various THz imaging techniques, THz tomography [1,2] can visualize internal structures of an object as a cross sectional image. THz tomography is realized by a time-of-flight measurement of THz echo pulses when a THz pulse is incident upon a sample in a reflection configuration. The internal structure of the sample can then be visualized from the distribution of the group refractive index. Since THz tomography acts as a noncontact and nonionizing

probe, in contrast to ultrasound and x ray methods, it has been used to visualize the cross section of internal structures in various applications, such as for floppy disks [2], pharmaceutical tablet coatings [3], skin burn [1], and skin cancer [4].

Another interesting application of THz tomography is nondestructive testing of paint film. The painting of industrial products, such as cars, ships, and aircraft, is important for rust prevention, waterproofing, color effects, light weight, and so on. Hence, quality control of the paint film using a paint meter (test equipment for measuring painting thickness) is required to maintain these functions. Furthermore, in certain industries, such as the car industry, in-process monitoring methods for paint films are required to control the painting spray in real time based on monitoring results, to achieve strict quality control of the paint film. In the field of nondestructive testing of paint film, many methodologies have been established. Contact-type thickness meters with handheld scanners, such as ultrasonic testing [5] and eddy-current testing [5], are powerful tools for simple and portable applica-

tions. However, these meters have limitations with regard to the quality of the material of the paint films and substrates, multilayered paint, wet paint, mapping of thickness distribution, and/or detection of painting defects [6]. Furthermore, contact-type thickness meters cannot be applied to in-process monitoring because the in-process monitoring requires remote measurement of paint thickness. The photothermal method [7] is suitable for the remote measurement at high spatial resolution. However, since this method is based on the temporal behavior of heat injected by light, it is difficult to apply to wet paint films that might be affected by heat. This limits its use in in-process paint monitoring.

We have previously proposed a THz paint meter based on THz tomography, as a noncontact tool for testing paint films [6]. This method is applicable to investigating various kinds of paint films and substrates, multilayered paint, mapping of thickness distribution, and/or detecting painting defects. Since the THz paint meter uses THz pulses with low average power (typically, nW to  $\mu$ W), it can measure wet paint films without causing effects due to heat induced by the THz pulse. Monitoring of the dryness in wet paint films has been demonstrated through the spectroscopic difference in the THz region between wet and dry paint films. However, since THz tomography is typically based on point-by-point measurements, it is necessary to perform two-dimensional mechanical scanning of the time delay and sample position to construct a two-dimensional tomographic image of the sample. The resultant high time consumption of this method has limited its application to stationary objects. Recently, we proposed real-time two-dimensional THz tomography to shorten the measurement time drastically, and demonstrated the technique in a THz paint meter for real-time monitoring of the paint film of a moving object and the drying progress of a wet paint film [8]. The availability of real-time monitoring makes THz paint meters attractive for in-process paint monitoring.

An unsolved problem for in-process paint monitoring is that the minimum thickness of the THz paint meter is insufficient for measuring thin paint films used for car bodies (typically less than a few tens of  $\mu$ m). In the THz paint meter, when successive THz echo pulses are well separated in time (i.e., for a thick paint film), the thickness of the paint film can be determined with an accuracy of a few  $\mu$ m. However, when the successive THz echo pulses are close to each other and overlap (i.e., for a thin paint film), the time delay of the THz echo pulses is affected by the temporal overlap. Therefore, a numerical Fourier deconvolution process (i.e., division of the Fourier spectra of the incident and reflected waveforms with a low-pass filter to remove noise) is often applied to extract an impulse response signal from the THz echo pulse train [2,6]. This process produces a sharp spike at a time delay corresponding to the position of each reflecting interface. The duration of the spike is determined by the cut-off frequency of the low-pass filter, which is set to cover the frequency bandwidth of THz

radiation. In this case, the minimum thickness, determined by the spike duration, is constrained to be half the coherent length of the THz pulse in a sample. Although it is possible to generate a narrower spike by using a low-pass filter with a higher cut-off frequency, this increases the noise components at higher frequencies, and a weak THz echo pulse is buried under the noise. This results in a decrease of quantitative accuracy in thickness measurements of thin paint films, and therefore numerical Fourier deconvolution is not effective in improving the minimum thickness below half the coherent length of the THz pulse. A direct method to decrease the minimum paint thickness is to shorten the THz pulse duration. However, even though the pulse, duration of a femtosecond laser for THz generation can be varied in the range 50–200 fs, the THz electric field is not changed significantly. Broadband THz radiation generated by an even shorter femtosecond laser is no longer a monocycle pulse, but instead is a multicycle pulse [9], which is not suitable for THz tomography. Another method to decrease the minimum thickness is to use a numerical parameter fitting algorithm to separate superposed THz echo pulses, in place of numerical Fourier deconvolution. In multi-component spectrum analysis in which the spectra of each component overlap spectrally, a parameter fitting algorithm based on multiple-regression analysis is often used to separate the spectra [10,11]. Multi-component spectrum analysis is analogous to the case of successive THz echo pulses close to each other and overlapping temporally (when applying a THz paint meter to a thin paint film).

In this paper, we present a method to decrease the minimum thickness of a THz paint meter using a parameter fitting method based on multiple-regression analysis. We apply the parameter fitting method to the monitoring of the optical thickness, geometrical thickness, and group refractive index of dry paint film and wet paint film.

## 2. Principle

We consider a single-layer paint film on a metal substrate, as shown in Fig. 1. When numerical Fourier deconvolution is used for a THz paint meter, the minimum paint thickness ( $d_{\min}$ ) is determined to be as follows [6]:

$$d_{\min} = (c\Delta T)/(2n_g), \quad (1)$$

where  $c$  is the velocity of light in vacuum,  $\Delta T$  is the temporal width of the THz pulse, and  $n_g$  is the group refractive index of the paint film. The  $d_{\min}$  value is equal to half the coherent length of the THz pulse in the paint film. When the geometrical thickness of the paint film ( $d$ ) is sufficiently larger than  $d_{\min}$ , the two THz echo pulses returning from the front and rear surfaces of the paint film are well separated in time. The  $d$  value is determined by the time separation between the two echo signals ( $\Delta t$ ) and the  $n_g$  value as

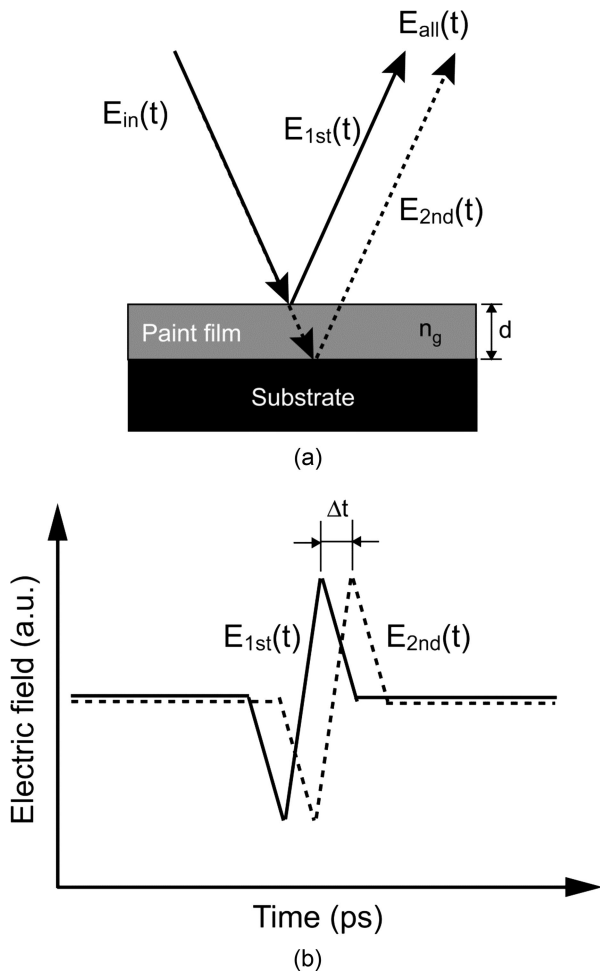


Fig. 1. Principle of the THz paint meter. (a) Single-layer paint film and (b) temporal waveforms of THz echo pulse.

follows:

$$d = (c\Delta t)/(2n_g). \quad (2)$$

However, when  $d < d_{\min}$ , the two THz echo pulses are not well separated and are superposed in time. In this case, it is difficult to determine  $d$  from  $\Delta t$  correctly because the degree of the temporal overlap changes the value of  $\Delta t$ .

We next consider the first and second THz echo pulses [ $E_{1st}(t)$  and  $E_{2nd}(t)$ ] returning from the front and rear surfaces of the paint film. In the following discussions, we neglect the effect of dispersion in the refractive index and absorption of the paint because the effect of dispersion is very small in a thin film. We also neglect the effect of multiple reflections of the THz pulse in the paint film for simplicity of the parameter fitting calculation.  $E_{1st}(t)$  and  $E_{2nd}(t)$  are expressed as follows:

$$E_{1st}(t) = R \times E_{in}(t + \Delta t_1), \quad (3)$$

$$E_{2nd}(t) = (1 - R)^2 \times \exp(-2d \times A) \times E_{in}(t + \Delta t_2) \approx \alpha \times E_{in}(t + \Delta t_2), \quad (4)$$

where  $E_{in}(t)$  is the incident THz pulse,  $R$  is the reflectivity at the paint surface,  $A$  is the absorption in the paint film, and  $\alpha$  is a parameter unifying the effects of surface reflection, absorption, and thickness of the paint film;  $\Delta t_1$  and  $\Delta t_2$  are the time delays of the first and second echoes in the paint film from  $E_{in}(t)$ , respectively. The difference between them ( $\Delta t_2 - \Delta t_1$ ) corresponds to the optical thickness ( $n_g d$ ) of the paint film, from which the geometrical thickness ( $d$ ) can be determined if  $n_g$  is known. The overall signal of the THz echo pulses [ $E_{all}(t)$ ] is expressed as:

$$E_{all}(t) = E_{1st}(t) + E_{2nd}(t) \approx R \times E_{in}(t + \Delta t_1) + \alpha \times E_{in}(t + \Delta t_2). \quad (5)$$

$R$ ,  $\alpha$ ,  $\Delta t_1$ , and  $\Delta t_2$  can be calculated by parameter fitting for measured  $E_{all}(t)$  and  $E_{in}(t)$  based on Eq. (5). In this way, the paint thickness can be determined from the calculated  $\Delta t_1$  and  $\Delta t_2$ , even though the two THz echo pulses overlap significantly. To this end, we perform multiple-regression analysis with the least-squares method to minimize the residual sum of the squares between a measured  $E_{all}(t)$  and a simulated  $E_{all}(t)$ . We then use the calculated  $\Delta t$  ( $= \Delta t_2 - \Delta t_1$ ) to determine the paint thickness based on Eq. (2).

### 3. Experimental Setup

A typical setup for THz tomography based on point-by-point measurements was prepared, as shown in Fig. 2. The laser light from a mode-locked (ML) Ti:sapphire laser oscillator (ML Ti:S laser; pulse duration = 100 fs, central wavelength = 800 nm, repetition rate = 80 MHz, average power = 1 W) is split into a pump light and a probe light with a beam splitter (BS). The pump light is focused by an objective lens (L) onto a dipole-shaped, low-temperature-grown GaAs photoconductive antenna for THz generation (THz-EM). To improve the signal-to-noise

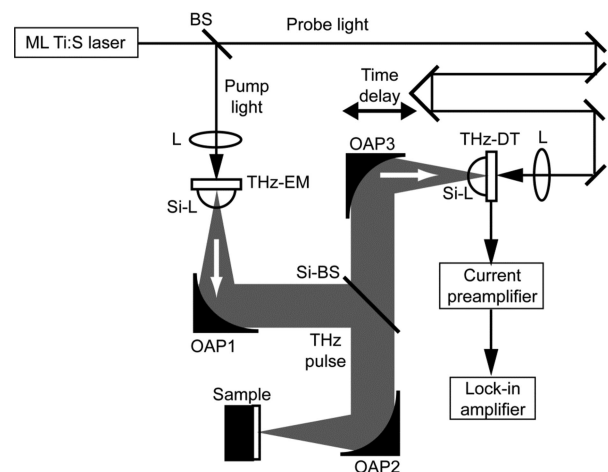


Fig. 2. Experimental setup. ML Ti:S laser: mode-locked Ti:sapphire laser; BS: beam splitter; L: objective lens; THz-EM: photoconductive antenna for THz generation; Si-L: hemispherical silicon lens; OAP1, OAP2, OAP3: off-axis parabolic mirrors; Si-BS: hemispherical silicon beam splitter; THz-DT: photoconductive antenna for THz detection.

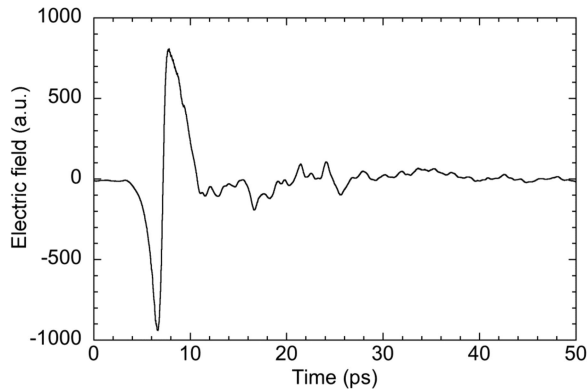


Fig. 3. Temporal waveform of an incident THz pulse  $[E_{in}(t)]$  obtained when setting an aluminum substrate at the sample position.

(S/N) ratio using lock-in detection, we chopped the THz pulse by electric bias modulation of the THz-EM (amplitude = 20 V<sub>p-p</sub>, offset = 10 V, freq. = 5 kHz [12]). The radiated THz beam is focused on a sample via a hemispherical silicon lens (Si-L), two off-axis parabolic mirrors (OAP1 and OAP2), and a silicon beam splitter (Si-BS). The THz echo pulse returned from the sample is recollimated and focused onto another dipole-shaped, photoconductive antenna for THz detection (THz-DT) with mirrors OAP2 and OAP3 and another Si-L. The effective focal lengths of OAP1, OAP2, and OAP3 are 76.2 mm. The probe light is incident on the THz-DT via a motor-driven-mechanical delay line. When the THz pulse and the probe pulse are incident on the THz-DT simultaneously, the electric field of the THz pulse causes a transient photocurrent in the THz-DT. The temporal waveform of the THz electric field is obtained with a lock-in amplifier (time constant = 100 ms) after passing through a current preamplifier. To determine the profile of  $E_{in}(t)$ , we set an aluminum mirror at the sample position and measured the temporal waveform of the THz electric field. We obtained a pulsed THz electric field with 1.2 ps pulse duration and an S/N ratio over 800, as shown in Fig. 3.

## 4. Results

### A. Dry Paint Film

As a sample we used an oil-based, acrylic paint film (black color) on an aluminum substrate. The group refractive index ( $n_g$ ) of the dry paint sample was determined beforehand using thick paint film samples from the relationship between the geometrical thickness ( $d$ ) measured with a contact-type thickness meter (eddy-current type, precision =  $\pm 3\%$  of the actual thickness) and the optical thickness ( $n_g d$ ) measured with a THz paint meter according to the procedure given in a previous paper [6]. The  $n_g$  value of the sample was determined to be 1.66, and  $d_{min}$  in the present system was estimated to be 108  $\mu\text{m}$  based on Eq. (1). We selected six single-layer dry paint film samples with different geometrical thick-

nesses ( $d = 60, 50, 40, 30, 20,$  and  $10 \mu\text{m}$ ), all less than  $d_{min}$ .

A temporal waveform of the THz echo pulses measured in the 60  $\mu\text{m}$  thick paint film is shown in Fig. 4(a). A comparison between Figs. 3 and 4(a) indicates that it is difficult to directly distinguish  $E_{1st}(t)$  and  $E_{2nd}(t)$  in the 60  $\mu\text{m}$  thick paint film. In the multiple-regression analysis with the least-squares method, the temporal waveform in Fig. 4(a) was used as an

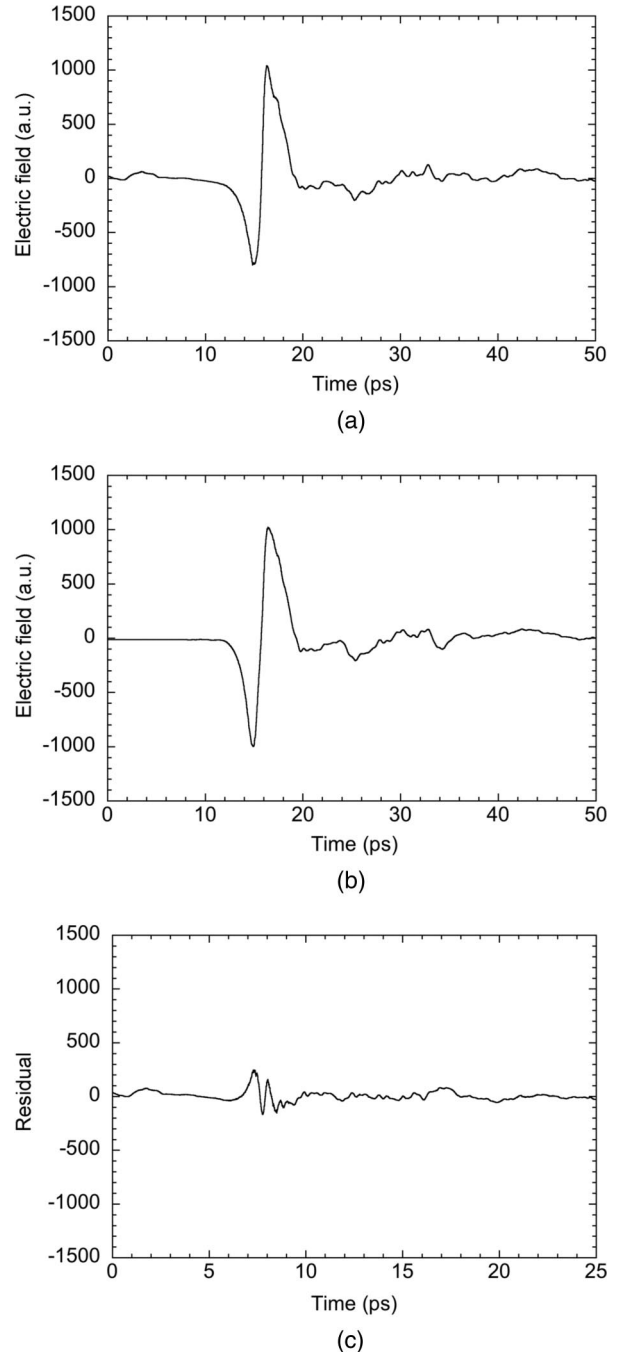


Fig. 4. Temporal waveform of the THz echo pulse of a single-layer dry paint film with 60  $\mu\text{m}$  thickness. (a) Signal measured with THz paint meter, (b) signal simulated by multiple-regression analysis, and (c) residual between the measured signal and simulated signal.

Table 1. Result of Multiple Regression Analysis for Dry Paint Films

Paint Thickness ( $\mu\text{m}$ )	$k_0$	$k_1$ (ps)	$k_2$	$k_3$ (ps)	Loop Number	$\Delta t$ (ps) [ $= k_3 - k_1$ ]	$d$ ( $\mu\text{m}$ )
60	0.44	8.091	0.56	8.774	5	0.683	61
50	0.48	2.144	0.52	2.682	2	0.538	48
40	0.48	8.501	0.52	8.911	4	0.410	37
30	0.50	0.850	0.50	1.190	3	0.340	31
20	0.50	2.745	0.50	3.008	10	0.263	23
10	NA	NA	NA	NA	NA	NA	NA

objective function  $X$ . We defined a model function  $Y$  to simulate the objective function  $X$  as follows:

$$Y = k_0 \times E_{in}(t - k_1) + k_2 \times E_{in}(t - k_3), \quad (6)$$

where  $t$  is an independent variable and  $k_i$  ( $i = 0, 1, 2, 3$ ) is a regression parameter. The following constraint conditions are applied for the regression parameters  $k_i$ :

$$\begin{aligned} k_0, k_2 &> 0 \\ k_1 &< k_3 \\ k_0 + k_2 &= 1. \end{aligned} \quad (7)$$

Before starting the multiple-regression analysis, we set the initial values  $k_0, k_1, k_2$ , and  $k_3$  to simulate  $X$  with as good an approximation as possible so that the analysis converges to a characteristic global minimum and not to incorrect local minima. The multiple-regression analysis was performed using computing software (IGOR PRO, WaveMetrics, Inc.) and was automatically repeated until the residual sum of the squares ( $\chi^2$ ) between  $X$  and  $Y$  reached the global minimum. Table 1 shows the result of the multiple-regression analysis for the 60  $\mu\text{m}$  thick paint film. Figures 4(b) and 4(c) show the simulated  $Y$  resulting from the multiple-regression analysis and the residual ( $\chi$ ) between  $X$  and  $Y$ , respectively. We can confirm from these results that the simulated  $Y$  well reproduces the measured  $X$ . The results for the other samples are also summarized in Table 1. We obtained good results for paint films with thicknesses of more than 20  $\mu\text{m}$ .

However, for the 10  $\mu\text{m}$  thickness paint film, the analysis did not converge even to a local minimum, let alone the global minimum, even though  $k_0, k_1, k_2$ , and  $k_3$  were varied over the whole available range. Hence, the present parameter fitting method is not applicable to paint films with thicknesses of less than 10  $\mu\text{m}$ . For the present experimental setup, this limitation is due to the THz pulse width ( $= 1.2$  ps) and the probe pulse width ( $= 100$  fs), because a paint thickness of 10  $\mu\text{m}$  is equivalent to a time separation of 111 fs.

For the parameter fitting algorithm, we consider that the minimum thickness is limited by two effects that were neglected in the analysis. One effect is

multiple reflections of the THz echo pulse in the paint film. When the Fresnel reflection at the paint surface is 0.25 from the group refractive indices of air ( $= 1$ ) and the paint ( $= 1.66$ ), the electric field of the THz echo pulse returning from the rear surface of the paint film is 56% of the THz incident pulse for no multiple reflections, 14% for one multiple reflection, and 3.5% for two multiple reflections. Although the effect of multiple reflections is neglected to simplify the parameter fitting calculation in this paper, for precise determination of the paint thickness the effect of multiple reflections must be considered. The second effect is the dispersion of the absorption and refractive index in the paint film. The dispersion effect distorts the temporal shape of the THz echo pulse. It is difficult to accurately apply the present fitting algorithm assuming that there is no temporal distortion of the THz echo pulse.

Figure 5 shows the relationship between the actual paint thickness ( $d$ ) determined by a contact-type thickness meter (eddy-current type, precision  $= \pm 3\%$  of the actual thickness) and that ( $d_{sim}$ ) simulated by multiple-regression analysis of each paint sample. The relationship between  $d$  and  $d_{sim}$  can be confirmed as being  $d = d_{sim}$  (fitting error:  $\chi^2 = 24, R = 0.986$ ),

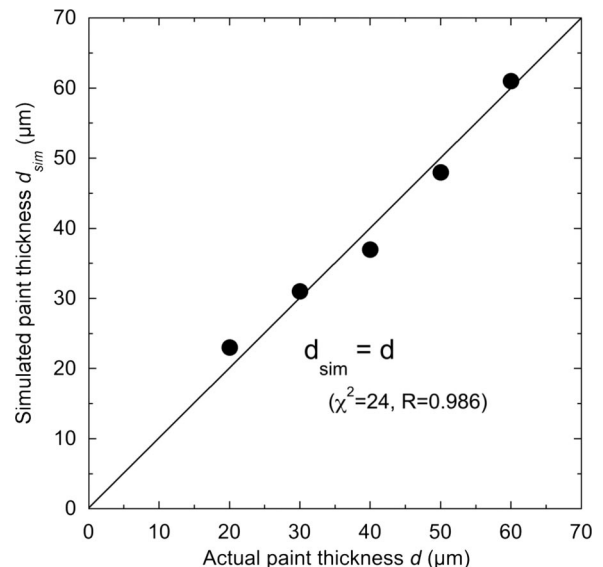


Fig. 5. Relationship between actual paint thickness measured with a contact-type thickness meter and simulated painting thickness by multiple regression analysis for five dry paint film samples with different thicknesses. Solid line represents  $d = d_{sim}$ .

and hence we can conclude that the minimum thickness of the present THz paint meter is correctly attained down to 20  $\mu\text{m}$  using multiple-regression analysis that improves the temporal resolution numerically. Defining the uncertainty as the standard deviation of the difference between  $d$  and  $d_{\text{sim}}$ , an uncertainty of 2.4  $\mu\text{m}$  was obtained. The uncertainty was due to the limitation of the present fitting method, the precision of the contact-type thickness meter, and the inconsistency of the measurement spot between the THz paint meter and the contact-type thickness meter.

We next investigated the effect of the S/N ratio in the measured THz echo signal ( $X$ ). The noise in the THz paint meter is due to two sources, environmental artifacts and background noise. When the THz paint meter is used in a factory environment, the main noise source is environmental artifacts, such as air turbulence or mechanical vibration. Conversely, in a stable condition with less environmental artifacts, background noise, such as the noise of the detector or amplifier, is dominant. The effect of the two types of noise on the THz signal is that different environmental artifacts have a multiplying effect, while background noise has an additive effect. Our objective for the THz paint meter is for use in a factory environment with various artifacts. Therefore, we successively decreased the S/N ratio to 40 for the THz echo signal ( $X$ ) measured in the 20  $\mu\text{m}$  paint film by multiplying the THz signal by white noise. We then determined the minimum  $\chi^2$  for  $X$  at each S/N ratio while varying  $k_0$ ,  $k_1$ ,  $k_2$ , and  $k_3$  over the available range to achieve accurate parameter fitting. Figure 6 shows the relationship between the S/N ratio and the simulated paint thickness. The simulated paint thickness converges well to the actual paint thickness (20  $\mu\text{m}$ ) when the S/N ratio  $> 100$ . However, when the S/N ratio  $< 100$ , the simulated values deviate significantly from the actual paint thickness. Therefore, an S/N ratio of more than 100 is required to

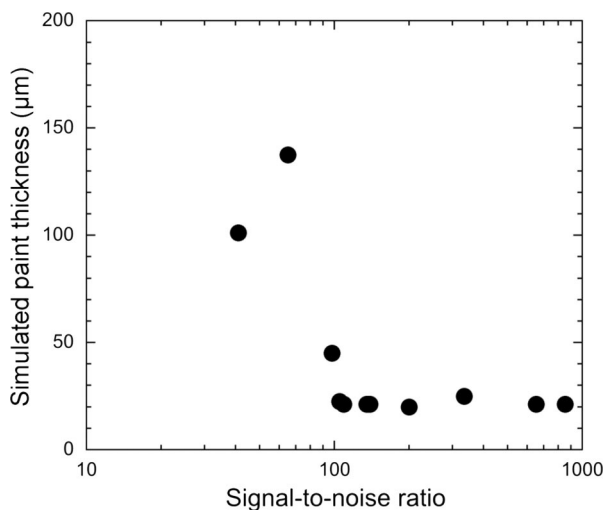


Fig. 6. Change of simulated paint thickness for the 20  $\mu\text{m}$  paint film when changing the S/N ratio.

determine the paint thickness correctly with the proposed parameter fitting method. This is because noise due to environmental artifacts is dependent on the electric field of the THz echo signal by a multiplicative factor, and is enhanced largely around the THz echo pulse. When adding white noise to the THz signal (i.e., simulating a stable condition with less environmental artifacts), the proposed fitting algorithm could be used at a lower S/N ratio. The THz paint meter can easily achieve an S/N ratio over 100 because the THz absorption of a paint film is low in general. Hence, the proposed method is useful for decreasing the minimum paint thickness in a THz paint meter.

We plot the  $k_0$  and  $k_2$  parameters with respect to each paint sample in Fig. 7. The  $k_0$  parameter should be fixed at a certain level for all the samples if the surface of each paint film is always placed at the same position with high precision. For example, the  $k_0$  parameter is calculated to be 0.25 from the Fresnel reflection formula for the group refractive indices of air ( $= 1$ ) and the paint ( $= 1.66$ ). The actual  $k_0$  parameter deviates greatly from this value and is not constant. The deviation and fluctuation are due to variations of the focal condition of the THz beam for each sample, caused by positioning imprecision and/or tilting of the sample. On the other hand, the  $k_2$  parameter is influenced by THz absorption of the paint film [see Eq. (4)]. If the THz absorption is dominant over variations of the focal condition of the THz beam, the  $k_2$  parameter will be dependent on the paint thickness. However, the actual  $k_2$  parameter is independent of the paint thickness, which implies that THz absorption in the paint film is negligible. We consider that the  $k_0$  and  $k_2$  parameters act as buffers to cancel the fluctuation of the focal condition of the THz beam. Since the paint thickness can be determined by the  $k_1$  and  $k_3$  parameters, the number of fitting parameters can be reduced for faster convergence of the multiple regression analysis. This will expand the range of measurable film thickness.

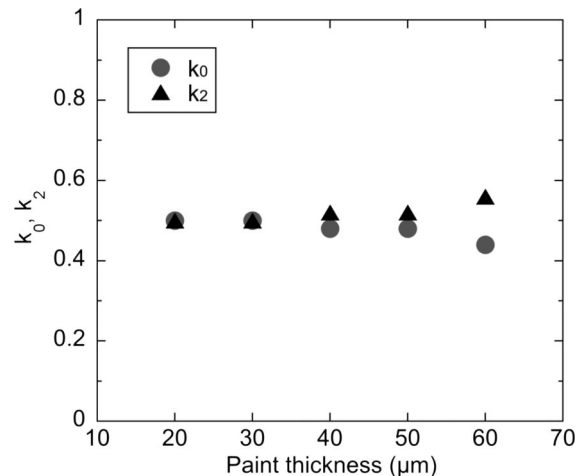


Fig. 7. Parameters  $k_0$  and  $k_2$  for five dry paint film samples with different thickness.

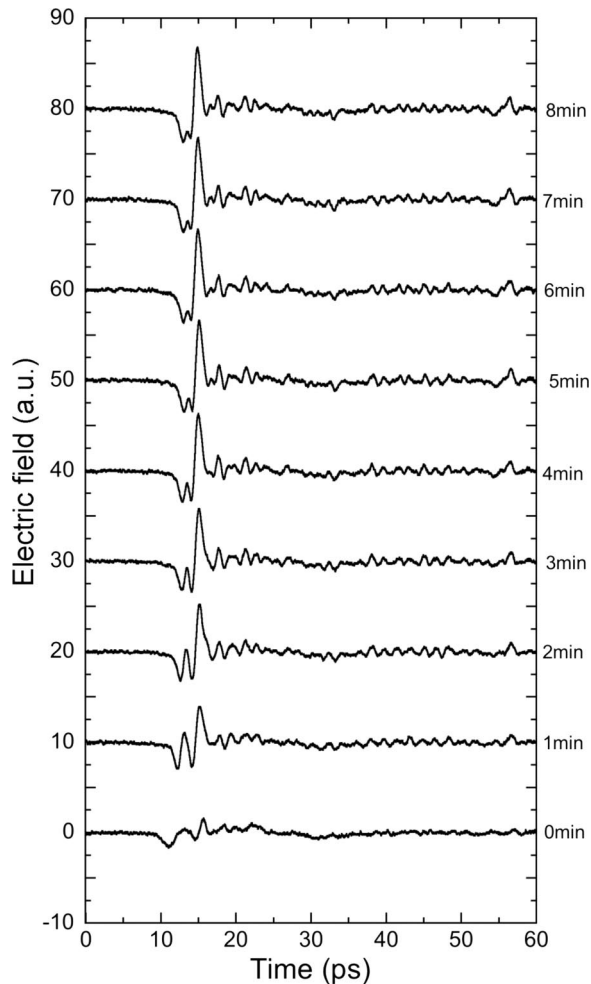


Fig. 8. Temporal evolution of THz echo pulse signal during the wet-to-dry transformation of a paint film. Temporal waveforms of the THz echo pulses were measured every 1 min after applying the paint.

### B. Wet Paint Film

An advantage of a THz paint meter over a conventional thickness meter is the ability to monitor dryness and paint thickness of a wet paint film. There is a discernible difference in the spectroscopic characteristics (index of refraction and absorption) in the THz range between the wet and dry conditions of paint film, and therefore the wet-to-dry transforma-

tion causes a temporal change of the THz echo pulse train [6,8]. We previously reported that two echo pulses, from the paint surface and the paint-substrate boundary, temporally evolve in time delay and pulse height. We further proposed time delay and echo pulse contrast as drying degree parameters, which can be directly extracted from the THz echo pulse signal. However, the two echo pulses for a thin wet paint film are not well separated and overlap in time. Such a temporal overlap of two THz echo pulses may lead to errors in the parameters. Therefore, we applied the parameter fitting method described in Subsection 4.A to the correct monitoring of dryness and paint thickness in a thin wet paint film.

For this examination, we applied another black acrylic paint film (quick-drying type) on an aluminum substrate just before starting the measurement. We then measured the temporal waveform of THz echo pulses every 1 min after applying the paint. Figure 8 shows the temporal evolution of the THz echo pulse signal. The first echo comes from the paint surface while the second echo is a reflection from the paint-substrate boundary. The time separation between the first and second echoes corresponds to the optical thickness of the paint film. We can confirm that the two echo pulses are separated before 2 min but overlap after 3 min. We applied the multiple-regression analysis based on Eq. (6) for the THz echo pulse signal of the wet paint film in Fig. 8. The results of the multiple-regression analysis, time delay ( $= \Delta t = k_3 - k_1$ ), and optical thickness ( $= c \cdot \Delta t / 2 = n_g d$ ) of the wet paint film are summarized in Table 2. If the group refractive index ( $= n_g$ ) is known, one can determine the geometrical thickness ( $= d$ ) from the optical thickness. However, in the case of the wet paint film, the group refractive index is unknown because it varies every moment depending on the drying degree. Therefore, it is impossible to determine the geometrical thickness from the optical thickness. However, if we utilize a relationship between geometrical thickness change and optical thickness change accompanying the wet-to-dry transformation, it is possible to determine the group refractive index of the wet paint film at each degree of the drying. Figure 9(a) shows the temporal changes of the  $k_1$  and  $\Delta t$  parameters with respect to the elapsed time, plotting their deviations from the initial values at 0 min. Since the

Table 2. Result of Multiple Regression Analysis for a Wet Paint Film

Elapsed Time (min)	$k_0$	$k_1$ (ps)	$k_2$	$k_3$ (ps)	Loop Number	$\Delta t$ (ps) [= $k_3 - k_1$ ]	$n_g d$ ( $\mu\text{m}$ )
0	0.44	-0.133	0.56	0.823	6	0.956	143
1	0.40	0.051	0.60	0.814	6	0.763	115
2	0.37	0.120	0.63	0.774	4	0.654	98
3	0.36	0.153	0.64	0.743	7	0.589	88
4	0.35	0.253	0.65	0.804	11	0.551	83
5	0.34	0.187	0.66	0.715	7	0.529	79
6	0.34	0.187	0.66	0.708	5	0.521	78
7	0.33	0.167	0.67	0.681	5	0.515	77
8	0.32	0.153	0.68	0.653	5	0.500	75

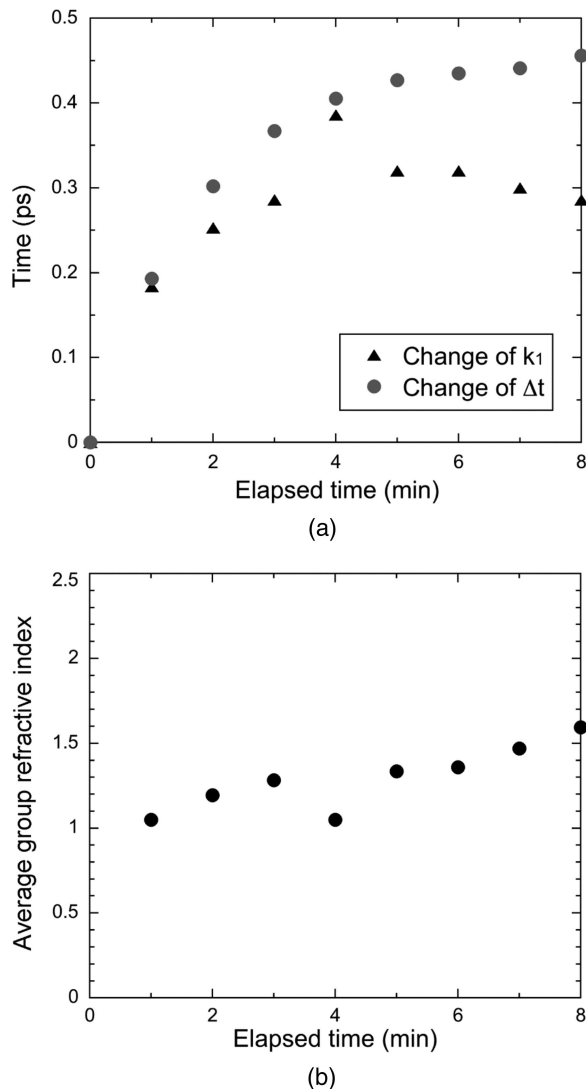


Fig. 9. Temporal change of each parameter for wet paint film with respect to elapsed time. (a) Deviations of  $\Delta t$  and  $k_1$  from the initial values at 0 min and (b) average group refractive index.

change of  $k_1$  is due to displacement of the paint surface caused by geometrical shrinkage, it is related to change of the geometrical thickness [=  $\Delta d_{\text{geo}}(t)$ ]. On the other hand, the change of  $\Delta t$  reflects that of optical thickness of the wet paint film [=  $\Delta d_{\text{opt}}(t)$ ]. The  $\Delta d_{\text{opt}}(t)$  is related with the  $\Delta d_{\text{geo}}(t)$  as follows:

$$\Delta d_{\text{opt}}(t) = N_g(t) \cdot \Delta d_{\text{geo}}(t), \quad (8)$$

where  $N_g(t)$  is an average group refractive index. With regard to the group refractive index of the wet paint film, we have to consider its inhomogeneity along the depth direction because the drying advances from the paint surface. Therefore, we use the average group refractive index  $N_g(t)$  for the wet paint film. From Eq. (8) and the results of Fig. 9(a), we determined the average group refractive index of the wet paint film at each degree of the drying, as shown in Fig. 9(b). We consider that the large fluctuation of the average group refractive index at 4 min is due to

an error in the parameter fitting method, indicating too many loop numbers as compared with other fitting results. It is clear from Figs. 9(a) and 9(b) that the wet-to-dry transformation changes the optical thickness, geometrical thickness, and average group refractive index of the wet paint film.

The average group refractive index is effective for monitoring of the dryness of the wet paint film. In general, wet paint is composed of a resin (e.g., acrylic resin), a pigment, and an organic solvent (e.g., paint thinner). The drying process of the wet paint is temporally advanced by the volatilization of the organic solvent, and the volatilization of the solvent and/or chemical change of the resin caused the spectroscopic difference in the THz region between the wet and dry conditions of a paint film. For example, since the wet paint has the group refractive index dominated by the solvent, the group refractive index of the wet paint film is smaller than that of the dry film and thus it increases depending on the degree of drying. If the group refractive index of the dry paint film is known, the difference of the group refractive index between the wet and dry paint films indicates the dryness of the wet paint. Therefore, the average group refractive index of the wet paint film can be used as a quantitative parameter indicating the drying progress. Since the group refractive index of the black acrylic paint used is 1.81 for dry film [6], temporal change of the average group refractive index in Fig. 9(b) indicated that the drying process is not still completed at 8 min.

## 5. Conclusions

We proposed a numerical parameter fitting method based on multiple-regression analysis to separate superposed THz echo pulses in a THz paint meter. The minimum paint thickness for a THz paint meter was decreased from 108 to 20  $\mu\text{m}$  at an S/N ratio of over 100 by the use of multiple-regression analysis. A parameter fitting method considering multiple reflections of the THz echo pulse and/or the dispersive absorption and refractive index in a paint film will further decrease the minimum paint thickness to less than 20  $\mu\text{m}$ .

We applied the proposed parameter fitting method to determining the optical thickness and group refractive index of a wet paint film. The results indicate that optical shrinking occurs, caused by both geometrical shrinking and a change in the group refractive index in the wet-to-dry transformation of the paint film. The proposed method will be useful for decreasing the minimum thickness for THz paint meters and other THz tomography measurements.

This work was supported by the Industrial Technology Research Grant Program 2002 of the New Energy and Industrial Technology Development Organization (NEDO) of Japan, the Strategic Information and Communications R&D Promotion Program (SCOPE) of the Ministry of Internal Affairs and Communications (MIC) of Japan, and Grants-in-Aid for Scientific Research 18686008 and 18650121 from the Ministry

of Education, Culture, Sports, Science, and Technology of Japan. We are grateful to Mamoru Hashimoto of Osaka University for fruitful discussions.

## References

1. D. M. Mittleman, R. H. Jacobsen, and M. C. Nuss, "T-ray imaging," *IEEE J. Sel. Top. Quantum Electron.* **2**, 679–692 (1996).
2. D. M. Mittleman, S. Hunsche, L. Boivin, and M. C. Nuss, "T-ray tomography," *Opt. Lett.* **22**, 904–906 (1997).
3. A. J. Fitzgerald, B. E. Cole, and P. F. Taday, "Nondestructive analysis of tablet coating thicknesses using terahertz pulsed imaging," *J. Pharm. Sci.* **94**, 177–183 (2005).
4. R. M. Woodward, B. E. Cole, V. P. Wallace, R. J. Pye, D. D. Arnone, E. H. Linfield, and M. Pepper, "Terahertz pulse imaging in reflection geometry of human skin cancer and skin tissue," *Phys. Med. Biol.* **47**, 3853–3863 (2002).
5. D. E. Bray and D. McBride, *Nondestructive Testing Techniques* (Wiley, 1992).
6. T. Yasui, T. Yasuda, K. Sawanaka, and T. Araki, "A terahertz paint meter for noncontact monitoring of thickness and drying progress in paint film," *Appl. Opt.* **44**, 6849–6856 (2005).
7. G. Busse, D. Wu, and W. Karpen, "Thermal wave imaging with phase sensitive modulated thermography," *J. Appl. Phys.* **71**, 3962–3965 (1992).
8. T. Yasuda, T. Yasui, T. Araki, and E. Abraham, "Real-time two-dimensional terahertz tomography of moving objects," *Opt. Commun.* **267**, 128–136 (2006).
9. Q. Wu and X.-C. Zhang, "Free-space electro-optics sampling of mid-infrared pulses," *Appl. Phys. Lett.* **71**, 1285–1286 (1997).
10. J. A. Blackburn, "Computer program for multicomponent spectrum analysis using least-squares method," *Anal. Chem.* **37**, 1000–1003 (1965).
11. D. J. Leggett, "Numerical analysis of multicomponent spectra," *Anal. Chem.* **49**, 276–281 (1971).
12. T. Yasui and T. Araki, "Dependence of terahertz electric field on electric bias and modulation frequency in pulsed terahertz emission from electrically modulated photoconductive antenna detected with free-space electro-optic sampling," *Jpn. J. Appl. Phys., Part 1* **44**, 1777–1780 (2005).